

Dynamical phase quantum thermometer for an ultracold Bose-Einstein Condensate

Carlos Sabin,¹ Angela White,^{1,2} Lucia Hackermuller,³ and Ivette Fuentes¹

¹*School of Mathematical Sciences, University of Nottingham,
University Park, Nottingham NG7 2RD, United Kingdom*

²*Joint Quantum Centre (JQC) Durham-Newcastle,
School of Mathematics and Statistics, Newcastle University,
Newcastle upon Tyne, NE1 7RU, United Kingdom*

³*School of Physics and Astronomy, University of Nottingham,
University Park, Nottingham NG7 2RD, United Kingdom*

We introduce a primary thermometer which measures the temperature of a Bose-Einstein Condensate ranging from the sub nK regime to the condensate critical temperature. We show, using Fisher information, that the precision of our technique improves the state of the art in thermometry. The temperature of the condensate is mapped onto the quantum phase of an atomic dot that interacts with the system for short times. We show that the highest precision is achieved when the phase is dynamical rather than geometric and when it is detected through Ramsey interferometry. Entanglement among several atomic dots can be used to further improve the precision and reach the Heisenberg limit. Standard techniques to determine the temperature of a condensate involve an indirect estimation through mean particle velocities made after releasing the condensate. In contrast to these destructive measurements, our method involves a negligible disturbance of the system.

Temperature is a crucial concept in quantum physics. Paradigmatic phenomena such as superconductivity and Bose-Einstein condensation only occur below a critical temperature. Bose Einstein Condensates (BECs) [1] allow the study of quantum effects in systems consisting of up to 10^8 atoms by cooling them to regimes in which the individual atomic wavefunctions overlap. In this case, the system exhibits quantum behaviour at mesoscopic scales. Very low temperatures are also required to observe quantum field theory effects e.g. Unruh-Hawking radiation [2].

Quantum field theory predicts that the dynamics of spacetime or the presence of horizons produce quantum particles from vacuum fluctuations. For example, in the dynamical Casimir effect, a moving boundary condition gives rise to vacuum excitations. This effect was recently demonstrated in superconducting circuits [3]. Currently several experimental groups in the field of analogue gravity attempt to demonstrate cosmological particle creation, dynamical Casimir effect and Hawking radiation in analogue spacetimes produced in BECs [4]. However, in a BEC a thermal background is always present due to unavoidable atomic collisions. In experiments, it is crucial to work at low temperatures so that the quantum particles created by effects of emergent spacetimes can be distinguished from this thermal noise. Recent experiments to demonstrate the dynamical Casimir effect in a BEC [4], have not been able to ensure that the excitations produced are indeed quantum even at temperatures as low as 200 nK. A method to accurately determine temperatures in the nK regime would be of great benefit to these experiments.

The temperature of a BEC is commonly estimated indirectly by comparing the density profile of the atoms with a classical Maxwell-Boltzmann velocity distribution [1, 5]. This density profile is determined by absorption imaging which is a destructive method that involves releasing the condensate. The relative errors in the measurement can be as high as $\sim 20\%$ [6]. Phase-contrast imaging [7] might be an alternative method to determine the temperature through the phase shift of a probe laser beam due to the interaction with the sample. However, at very low temperatures the method has low spatial resolution and can only be applied reliably if the condensate is allowed to freely expand for a given time [8]. Indeed absorption imaging is the standard technique for measuring temperatures in the nK regime [6] and, in general, for probing the condensate [9]. From a more fundamental viewpoint, it is also natural to ask if it is appropriate to measure temperatures in a quantum regime using a method which involves a classical velocity distribution.

Recent theoretical and experimental developments in cold atom gases have lead to the experimental demonstration of systems consisting of mixtures of two different atomic species or two hyperfine states of the same species [10–14]. The number of particles in each component of the mixture is determined by the interatomic interactions which can be modulated experimentally, through a Feshbach resonance [13–15]. In particular, atomic quantum dots with only a single atom in a tight trap provided by a laser beam can be achieved within a condensate [16–20]. In this paper we show how an atomic quantum dot immersed within the condensate can be used to measure the temperature of the condensate with high precision and a negligible disturbance of the system. The scheme can be implemented using an optical lattice with a single atom per site, where each atom interact at a different time with the condensate [21]. This constitutes a primary thermometer which measures the temperatures ranging from the sub nK regime to the condensate critical temperature.

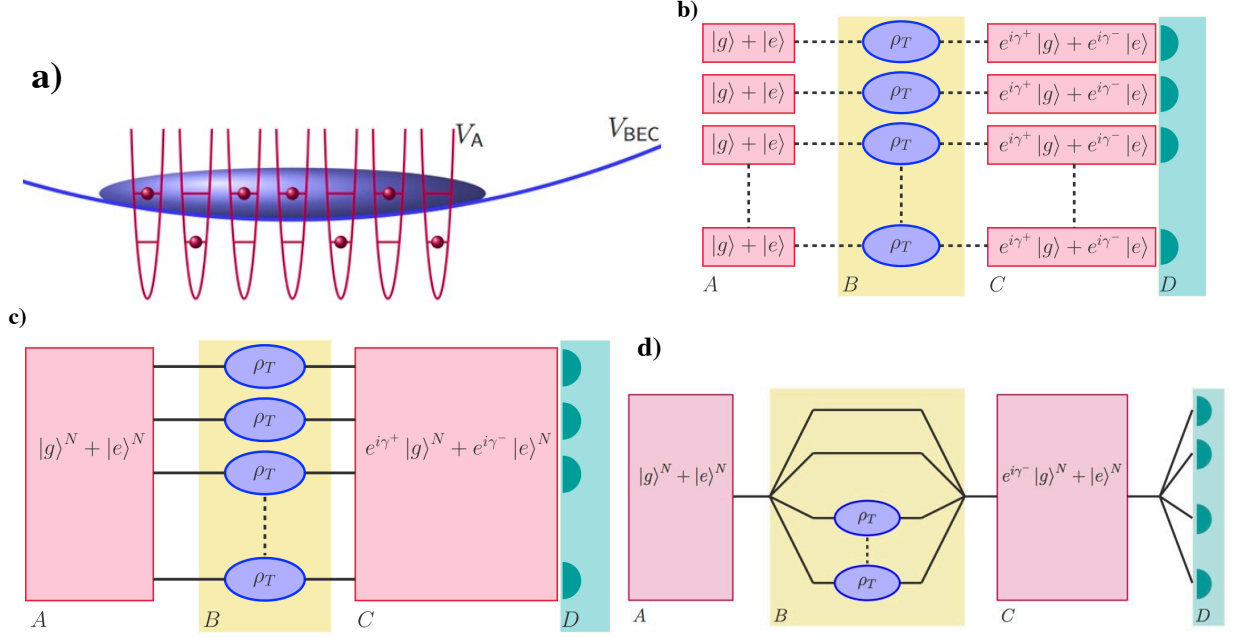


FIG. 1: a) Sketch of the experimental setup: several atomic quantum dots are embedded within a BEC reservoir. They are coupled at different times through a Raman transition to the phononic fluctuations of the BEC. b) Ramsey interferometry scheme to measure the dynamical phase and hence measure temperature. c) Ramsey interferometry scheme with entangled input states. d) Mach-Zehnder interferometer scheme with entangled input states. A. Input state, B. Interaction switched on, C. Final state D. Readout

Results We start by showing how a two-level system interacting with a quantum field in a thermal state through the standard Jaynes-Cummings Hamiltonian can acquire a dynamical phase that depends on the temperature of the field. This phase is then read out through Ramsey interferometry. We estimate the precision of this procedure by computing the Quantum Fisher Information. Finally, we give details of possible physical implementations of the thermometer using atomic quantum dots or an optical lattice coupled to phonons in a BEC (see Fig.1). In both cases, the atoms must interact at different times with the condensate to ensure statistical independence. We show that with realistic experimental parameters, our thermometer precision improves on state of the art thermometry after a small number of measurements, where in this case, each dot embedded within the condensate or loaded into the optical lattice provides one measurement. In the case where the dots are prepared in an entangled state, the precision can reach the Heisenberg limit, that is the limit imposed fundamentally by quantum theory.

We now proceed to introduce our methods and results. We consider the Jaynes-Cummings model that describes the interaction of a two-level system of frequency gap Ω_d and one mode of a quantum field with frequency Ω_a

$$H_{JC}(t) = \hbar\Omega_a a^\dagger a + \hbar\frac{\Omega_d}{2}\sigma_z + \hbar g(\sigma^- a^\dagger e^{i\theta} + \sigma^+ a e^{-i\theta}), \quad (1)$$

where a, a^\dagger are creation and annihilation field operators, $\sigma^\pm = (1/2)(\sigma_x \pm i\sigma_y)$ and σ_x and σ_y are Pauli matrices. The coupling strength between the field and atom is given by g , the detuning is $\delta = |\Omega_a - \Omega_d|$ and the phase $\theta = kx - \delta t$ is a function of time and the position x of the atom. Later on, we will show under which circumstances an atomic dot interacting with the phonon field of a BEC can be reduced to this simple interaction.

The temperature of the field will be determined through the phases acquired by the atom through its evolution under the Hamiltonian (1), assuming the adiabatic approximation (see Appendix A). The total phase can be split into a geometric and a dynamical part. It has been shown that the geometric phase can be used to gain information about the quantum state of a bosonic field. For pure field states, the phase encodes information about the number of particles in the field [22]. In particular, for initial squeezed states, the phase depends also on the squeezing strength [23]. More recently, the geometric phase was also employed to estimate the temperature of the field [24]. We will show, using Quantum Fisher Information, that the dynamical phase is more convenient to estimate temperatures. We are interested in the case where the field is initially in a thermal state $\rho_F = \sum_n p_n |n_f\rangle \langle n_f|$, where $p_n = (e^{-F})^n (1 - e^{-F})$,

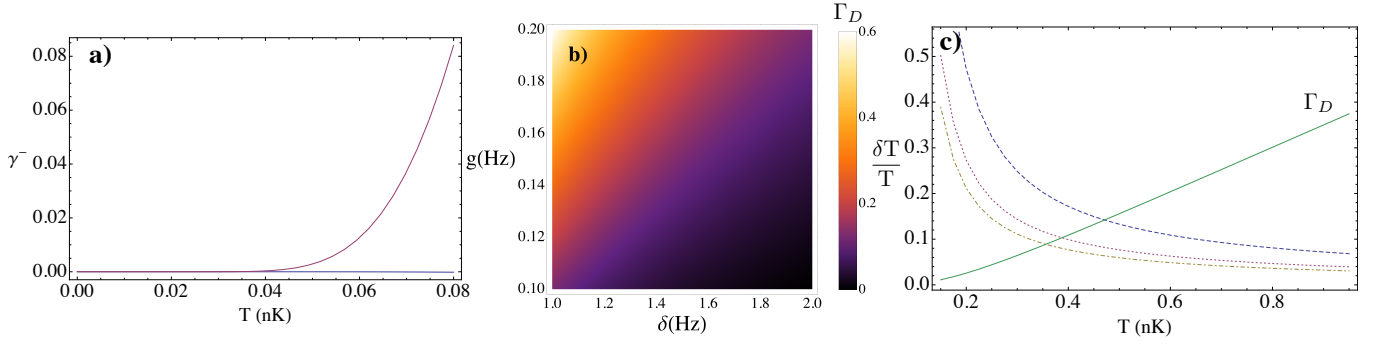


FIG. 2: a) Comparison of geometrical (solid, blue) γ_G^- vs. dynamical γ_D^- with $\Omega_a = 2\pi \times 10$ Hz, $g = 2\pi \times 0.2$ Hz, $\delta = 2\pi \times 2$ Hz and $c = 5$ mm/s. b) Dependence of the dynamical phase Γ_D with g and δ at $T = 0.5$ nK c) Γ_D (green, solid) and relative error $\delta T/T$ after 1000 (blue, dashed), 3000 (red, dotted) and 5000 (yellow, dash-dotted) measurements. The parameters are the same as in a).

$F = \frac{\hbar \Omega_a}{k_B T}$. We find, that the geometric phase is

$$\gamma_G^- \simeq \frac{g^2}{\delta^2(e^F - 1)} \quad (2)$$

and the dynamical phase

$$\gamma_D^- \simeq \frac{4\pi g^2 e^{-F}}{\delta^2(1 - e^{-F})}. \quad (3)$$

Therefore, the dynamical phase is always larger than its geometric counterpart

$$\gamma_G^- < \gamma_D^-. \quad (4)$$

In Fig.2a) we plot the dynamical and geometric phases for realistic experimental parameters. One observes that for temperatures in the sub nK regime, the geometric phase is negligible in comparison to the dynamical phase. Furthermore, we will show that the precision obtained through the dynamical phase in the measurement of the temperature is higher than the precision attainable with the geometric one.

Measurement Since the phases acquired by the system are global and cannot be measured directly, it is necessary to setup an interferometric scheme that will allow us to measure relative phases. In particular, the geometric phase, used in [24] to estimate temperatures, can only be detected using a Mach-Zehnder interferometer. In this type of interferometer the qubit is split into two different trajectories. In this case the qubit can be made to interact with a thermal field only in one arm of the interferometer acquiring a relative phase that can be measured at the interferometer's output. Now we will use standard techniques of phase estimation in Quantum Metrology to estimate the precision of the temperature measurement in this experiment (see Appendix B).

We consider that in one arm of the Mach-Zehnder interferometer the qubit, initially in state $|g\rangle$, interacts with a field in state ρ_T . In the second arm we assume the qubit in state $|e\rangle$ does not interact with the field. Since, up to the first order in g/δ the state $|g\rangle\langle g| \otimes \rho_T \simeq \sum P_n |n-\rangle\langle n-|$, the relative phase at the output will therefore be $\gamma^- = \gamma_D^- + \gamma_G^-$. Assuming that the dynamical phase can be canceled [25], we calculate the Fisher information to estimate the precision on the temperature measurement through this phase. Since in this case $F(\rho_T) = (\partial_T \gamma_G^-)^2$, the Cramer-Rao bound in the geometric case employing Mach-Zehnder interferometry, denoted by δT_M^G , yields

$$\delta T_M^G \geq \frac{1}{\sqrt{M} \partial_T \gamma_G^-} > \frac{T \delta^2 (e^F - 2)}{\sqrt{M} F g^2}. \quad (5)$$

Here the bound is obtained using a series expansion in g/δ . Following the same procedure we find bounds to the Fisher information for the case where the temperature is measured using the dynamical phase:

$$\frac{T \delta^2 (e^F - 1)^2}{\sqrt{M} 8 \pi F g^2 e^F} < \delta T_M^D < \frac{T \delta^2 (e^F - 1)^2}{\sqrt{M} 4 \pi F g^2 e^F}. \quad (6)$$

From Eq. (5) and (6) it follows that the error in estimating the temperature using the dynamical phase is smaller $\delta T_M^D < \delta T_M^G$. Furthermore, using the dynamical phase allows us to simplify the setup by using Ramsey rather than Mach-Zehnder interferometry. Mach-Zehnder atomic interferometry represents a strong experimental challenge while Ramsey interferometry does not involve spatially splitting the atomic wave function to undergo different trajectories.

In Ramsey interferometry the two-level system is prepared in a superposition state, $|\uparrow\rangle = |g\rangle + |e\rangle$, and it is allowed to interact with the quantum field in a thermal state ρ_T during a time t . After the interaction the probability of finding the two-level system in the excited state depends on the dynamical relative phase, Γ_D , picked up by it. Under weak adiabatic evolution the state $|\uparrow\rangle \langle\uparrow| \otimes \rho_T \simeq \sum P_n(|n-\rangle + |n+\rangle)(\langle n-| + \langle n+|)$ acquires the relative phase, $\Gamma_D = \gamma_D^+ - \gamma_D^-$, which is very sensitive to the temperature in an ultralow regime such as nK. The Fisher information in this case is given by $F(\rho_T) = (\partial_T \gamma_D^+ - \partial_T \gamma_D^-)^2 = 4(\partial_T \gamma_D^-)^2$. Therefore, the precision in the temperature measurement is increased by a factor of 2 for Ramsey interferometry, i.e. $\delta T_R^D = (1/2)\delta T_M^D$.

In Fig. 2b we plot the dependence of Γ_D on the detuning δ and the coupling strength g for the relevant experimental regime that we consider below. Notice that the phase is sensitive to g/δ and it is essentially determined by this ratio and Ω_a . In Fig. 2c we plot the relative error $\delta T_R^D/T$ after 1000, 3000 and 5000 measurements. The relative error achieved is around 5 %, which improves the 10-20 % of the current state of the art thermometry in the sub nK regime.

Experimental implementation We now consider a realistic implementation of the above results. We will consider a system consisting of a BEC superfluid reservoir in a shallow confining trap interacting with either an array of atomic quantum dots or a deep optical lattice loaded with cold atoms [16, 26–28]. Our discussion applies to both, dots and atoms in a lattice. However for the sake of clarity in our presentation, we will focus on the quantum dot scenarios. In the absence of atomic collisions, the BEC can in principle reach absolute zero temperature. Under this assumption, the condensate is commonly described by a classical density function. However, collisions are always present and therefore, in the superfluid regime, the condensate is better described by a mean field classical background plus quantum fluctuations. The fluctuations, for frequencies lower than the so-called healing length, are given by a phononic quantum field operator $\Pi(\mathbf{x})$, which can be expanded in terms of Bogoliubov modes. Now we proceed to describe the quantum dots and their interaction with the phononic field. Each dot is created by applying a localised steep potential which traps atoms of either a different hyperfine state of the same atomic species as the BEC, or alternatively, a different atomic species. We choose a large collisional interaction strength g_{aa} inside each dot well, to guarantee that the occupation number in each site is either 0 or 1, giving rise to an array of two level systems. We also assume that the wells are deep and separated enough to neglect direct interaction between different sites [26].

The phonons and the dots can be coupled through a Raman transition. The effective Hamiltonian obtained under the above assumptions can be written as [16, 26]: $H = H_A + H_B + H_{AB}$. H_A is the free Hamiltonian of an array of M dots, which is given by $H_A = \sum_{i=1}^M \hbar \Omega_d \sigma_z^i / 2$. The frequency Ω_d is a function of the Raman frequency Ω and the number of atoms in the condensate [16]. H_B is the free Hamiltonian for the phonons $H_B = \sum_k \hbar \omega_k a_k^\dagger a_k$, where $\omega_k = c |\mathbf{k}|$ and c is the speed of sound. Finally, the interaction Hamiltonian is given by:

$$H_{AB} = -\hbar \delta' \sum_{i=1}^M \sigma_z^i + \hbar (g_{ab} - g_{bb}) \sum_{i=1}^M \Pi(\mathbf{x}^i) \sigma_x^i, \quad (7)$$

where \mathbf{x}^i is the position of the dot in the condensate. The coupling strengths between dot-condensate and condensate-condensate atoms are given by g_{ab} and g_{bb} , respectively. The frequency δ' is a function of g_{ab} , g_{aa} , the Raman frequency and the detuning. All the coupling strengths g_{ab} , g_{aa} and g_{bb} can be tuned with Feshbach resonances. In particular, we will consider that the strengths are tuned such that $\delta' = 0$. In this case the system is described by the spin-boson Hamiltonian [16], in which the structure of the reservoir is characterised by the spectral density. The ubiquity of physical systems that can be described by the spin-boson Hamiltonian directly illustrates that the thermometry technique we describe can be applied to a range of different physical systems.

Now, with suitable boundary conditions for the condensate trap -e. g. hard-wall or box potentials [29, 30]-, the energy separation of the phononic modes can be large enough to ensure that each two-level system is only effectively coupled to the mode with closest frequency to Ω_d . We denote this frequency by Ω_a and apply the Rotating wave Approximation (RWA). Assuming that each dot interacts with the condensate at different times, the Hamiltonian for each dot is given by Eq. (1), where now the dot-field coupling strength g is given by:

$$g = \sqrt{\frac{c k}{2 \hbar V g_{bb}}} (g_{ab} - g_{bb}), \quad (8)$$

where V is the condensate volume. The RWA holds for weak couplings and small detunings $\{g, \delta\} \ll \epsilon$ where $\epsilon = \Omega_a + \Omega_d$. Taking typical values $L = 500 \mu\text{m}$ and $c = 5 \text{ mm/s}$ and assuming $\lambda_f \simeq L$, the frequency of the phonons

is given by $\Omega_a = 2\pi \times 10$ Hz. With experimental data for the Feshbach resonances [13–15] the values of g can be tuned within a broad range from $2\pi \times 0.1$ Hz to $2\pi \times 10$ Hz. Taking g around 0.1 Hz and a detuning of $2\pi \times 1 - 2$ Hz we are consistent with both RWA and the adiabatic approximation. This is the range of parameters explored in the plots.

Discussion The description of the experiment is the following. The atomic dots are prepared in a separable superposition of their internal levels, $\otimes_{i=1\dots M} |\uparrow_i\rangle$. They are then coupled to the phonons through Raman transitions and allowed to interact with the BEC for some time, which in our plots is of the order of 0.1 s. The times can be made significantly shorter by relaxing the cyclicity condition, which we imposed in order to compare the dynamical phase analysis with the geometrical phase analysis. However, it is no longer necessary in this setting. The probabilities of excitation are then measured using standard imaging techniques [21]. In order to make sure that the measurements are completely independent, each dot must interact at different times with the condensate. Moreover, the separation in time between interactions should be large enough to rule out temporal correlations between the occupation numbers of the considered mode. These temporal correlations drop to 0 after a few ms for typical parameters [31]. Another way to ensure that different measurements are not correlated is to couple each dot to a different mode of the field. In this case, the interactions can be simultaneous, since each dot would probe a different thermal distribution with the same temperature. The only limitation to the number of probes is that the spatial separation must be larger than the healing length of the condensate in order to ensure no direct interaction between them [26]. Moreover, indirect interaction due to phonon exchange is proportional to g^2/δ , and therefore is negligible for times $t = 1/\delta$ and $g/\delta \ll 1$. Taking for instance a realistic separation between the dots of 300 nm and a condensate length of 500 μm , we can load 1500 impurities in an optical lattice. Since the lifetime of the condensate can be larger than 100 s it seems feasible to perform at least a few measurements on each dot. Therefore, as can be seen in Fig. 2c) the relative error is well below the 20 % state of the art ultracold thermometry [6], and ultrahigh precisions below 1 % can be achieved. Moreover, as explained above, by preparing several dots in an entangled input state [18, 32] the precision would be significantly improved reaching the Heisenberg limit.

The Unruh temperature can in principle be measured in our setting by accelerating the dots. The idea of demonstrating the Unruh effect in BECs was suggested with a different setup in [33]. Moreover, the use of a geometric quantum phase as an estimator of the Unruh temperature was proposed using a challenging experimental setup involving atom Mach-Zehnder interferometry [34]. We are currently working on implementing our technique to measure the Unruh effect in a BEC with higher precision. If a is the acceleration, the Unruh temperature is given by $T_U = \hbar a / (2\pi c k_B)$ which in our setup give rise to $T_U = 2.4$ nK for an acceleration of g -where g is the acceleration of gravity on the surface of the Earth. Accelerations of several g were achieved in recent experiments [21]. Therefore, with our method the detection of the Unruh temperature of the phononic BEC bath is clearly within reach of current technology.

We have shown that the quantum dynamical phase acquired by a two-level system interacting with a quantum field in a thermal state under the Jaynes-Cummings Hamiltonian can be used to measure the temperature of the field. Since the Jaynes-Cummings model successfully describes a number of different quantum systems, our ideas can be applied to measure the temperature in a great variety of physical setups, such as cavity QED, ion traps or circuit QED in a weak coupling regime. As a particularly interesting implementation we choose to present in this paper a cold atom setup. In particular, an atomic quantum dot is coupled to the phononic quantum fluctuations of a BEC. We compute the dynamical phase acquired by several independent dots in a Ramsey interferometry scheme and estimate the precision by means of the Quantum Fisher Information. We show that the phase is sensitive to temperatures in the sub nK regime and that the precision improves on state of the art thermometry after a number of measurements that can be achieved with current technology. Moreover, the precision can be improved by preparing entangled input states. In summary, we have introduced a non-invasive, accurate and quantum way of measuring ultralow temperatures in a Bose-Einstein Condensate. In addition to improving on state-of the art thermometry, these techniques provide an experimentally feasible method of measuring very-low temperatures arising in analogue gravity scenarios, paving the way for the detection of analogue Unruh and Hawking temperatures in BECs.

Appendices

Appendix A: Dynamical and geometrical phases The time evolution of the system can be found by writing $H_{JC}(t) = U(\theta)H_{JC}^0 U(\theta)^\dagger$ where $U(\theta) = e^{i\theta a^\dagger a}$ and $H_{JC}^0 = H_{JC}(x=0, t=0)$. The eigenstates of H_{JC}^0 , are given by $|n-\rangle = \cos(\frac{\alpha_n}{2})|(n+1)g\rangle - \sin(\frac{\alpha_n}{2})|ne\rangle$ and $|n+\rangle = \sin(\frac{\alpha_n}{2})|(n+1)g\rangle + \cos(\frac{\alpha_n}{2})|ne\rangle$ where $|ng\rangle$ and $|ne\rangle$ are the eigenstates of the free Hamiltonian (corresponding to $g=0$) and $\alpha_n = \arctan(\frac{2g\sqrt{n+1}}{\delta})$. In this notation $|n\rangle$ are field number states and $|g\rangle$ and $|e\rangle$ are the ground and excited states of the qubit. We require that the qubit only

acquires phases during its evolution. Therefore, to ensure that there are no transitions between the $U(\theta) |n\pm\rangle$ states, we make use of the adiabatic approximation [35] $\sum_m \frac{|\langle m|\dot{H}|n\rangle|}{E_m - E_n} t \ll 1$. In the Jaynes-Cummings model transitions are only possible between the eigenstates with same n , therefore the adiabatic condition yields $\frac{|\langle n+|\dot{H}|n-\rangle|}{E_{n+} - E_{n-}} t \ll \frac{gt}{2}$. For simplicity, we assume that the parameter θ undergoes a cycle, therefore the interaction time is $t = 2\pi/\delta$. The dynamical phase γ_{Dn}^\pm acquired by the state $|n\pm\rangle$ under this condition is given by

$$\begin{aligned} \gamma_{Dn}^\pm &= -\frac{1}{\hbar} \int_0^t \langle H \rangle_{n\pm} dt' = -\frac{E_n^\pm t}{\hbar} = \\ &= -\frac{2\pi}{\delta} \left(\Omega_a \left(n - \frac{1}{2} \right) \pm \sqrt{\delta^2 + 4g^2 n} \right). \end{aligned} \quad (9)$$

The geometric phase γ_{Gn}^\pm defined by [22]: $i\gamma_{Gn}^\pm = \int_0^{2\pi} \langle U^\dagger \partial_\theta U \rangle_{n\pm} d\theta$, yields $\gamma_{Gn}^+ = 2\pi(n - \cos^2(\frac{\alpha_n}{2}))$ and $\gamma_{Gn}^- = 2\pi(n - \sin^2(\frac{\alpha_n}{2}))$. We are interested in the case where the field is initially in a thermal state $\rho_F = \sum_n p_n |n_f\rangle \langle n_f|$, where $p_n = (e^{-F})^n (1 - e^{-F})$, $F = \frac{\hbar\Omega_a}{k_B T}$. In the mixed case, the geometric phase is given by $\gamma_G^\pm = \text{Arg}(\sum_n p_n e^{i\gamma_{Gn}^\pm})$ [36, 37], while in the dynamical case, the phase is obtained through a simpler expression $\gamma_D^\pm = \sum_n p_n \gamma_{Dn}^\pm$. We find, using a series expansion on g/δ , that the geometric phase is given by Equation (2) and the dynamical phase by Equation (3)

Appendix B: Quantum Fisher Information The quantum Cramer-Rao bound [38] states that the error δx in estimating a parameter x with M measurements on a state ρ_x that depends on x , is bounded by:

$$\delta x \geq \frac{1}{\sqrt{M F(\rho_x)}}, \quad (10)$$

$F(\rho_x)$ being the Quantum Fisher Information of the state. This inequality assumes that input states are separable, however, it has been shown that entangled states improve the $1/\sqrt{M}$ shot-noise scaling reaching the Heisenberg limit given by a $1/M$ scaling where M is the number of entangled particles. $F(\rho_x)$ can be written as [39]:

$$F(\rho_x) = 2 \sum_{nm} \frac{|\langle m | \partial_x \rho_x | n \rangle|^2}{\rho_m + \rho_n} \quad (11)$$

where $\rho_{m,n}$ are the matrix elements of ρ_x in an orthogonal basis in which ρ_x is diagonal: $\rho_x = \sum_n \rho_n |n\rangle \langle n|$. The terms in which both ρ_m and ρ_n are zero in the sum in Eq. (11) must be excluded.

Acknowledgements We are indebted to Tomi Johnson for his very helpful insights. The authors would like also to thank Gerardo Adesso, Mehdi Ahmadi, Michael Berry, Per Delsing, Göran Johansson, Tim Ralph, Enrique Solano and Daniel Oi for useful discussions and the financial support of EPSRC Bridging the gaps. C. S and I. F. acknowledge support from EPSRC (CAF Grant No. EP/G00496X/2 to I. F.) A. W. acknowledges funding from EPSRC grant No. EP/H027777/1.

-
- [1] C. J. Pethick and H. Smith, *Bose Einstein Condensation in dilute gases* (Cambridge University Press, 2004).
 - [2] D. E. Bruschi, N. Friis, I. Fuentes, and S. Weinfurter, ArXiv e-prints (2013), 1305.3867.
 - [3] C. M. Wilson, G. Johansson, A. Pourkabirian, M. Simoen, J. R. Johansson, T. Duty, F. Nori, and P. Delsing, *Nature (London)* **479**, 376 (2011).
 - [4] J.-C. Jaskula, G. B. Partridge, M. Bonneau, R. Lopes, J. Ruaudel, D. Boiron, and C. I. Westbrook, *Phys. Rev. Lett.* **109**, 220401 (2012).
 - [5] W. Ketterle and M. W. Zwierlein, Making, probing and understanding Bose-Einstein Condensates (in *Ultracold Femi Gases*, Proceedings of the International School of Physics Enrico Fermi, IOS Press Amsterdam, 2006).
 - [6] A. E. Leanhardt, T. A. Pasquini, M. Saba, A. Schirotzek, Y. Shin, D. Kielpinski, D. E. Pritchard, and W. Ketterle, *Science* **301**, 1513 (2003).
 - [7] R. Meppelink, R. A. Rozendaal, S. B. Koller, J. M. Vogels, and P. van der Straten, *Phys. Rev. A* **81**, 053632 (2010).
 - [8] J. Stenger, D. Stamper-Kurn, M. Andrews, A. Chikkatur, S. Inouye, H.-J. Miesner, and W. Ketterle, *Journal of Low Temperature Physics* **113**, 167 (1998), ISSN 0022-2291.
 - [9] T. van Zoest, N. Gaaloul, Y. Singh, H. Ahlers, W. Herr, S. T. Seidel, W. Ertmer, E. Rasel, M. Eckart, E. Kajari, et al., *Science* **328**, 1540 (2010).

- [10] G. Modugno, G. Ferrari, G. Roati, R. J. Brecha, A. Simoni, and M. Inguscio, *Science* **294**, 1320 (2001).
- [11] G. Modugno, M. Modugno, F. Riboli, G. Roati, and M. Inguscio, *Phys. Rev. Lett.* **89**, 190404 (2002).
- [12] K. Günter, T. Stöferle, H. Moritz, M. Köhl, and T. Esslinger, *Phys. Rev. Lett.* **96**, 180402 (2006).
- [13] A. Simoni, M. Zaccanti, C. D'Errico, M. Fattori, G. Roati, M. Inguscio, and G. Modugno, *Phys. Rev. A* **77**, 052705 (2008).
- [14] S.-K. Tung, C. Parker, J. Johansen, C. Chin, Y. Wang, and P. S. Julienne, *Phys. Rev. A* **87**, 010702(R) (2013).
- [15] C. Chin, V. Vuletić, A. J. Kerman, S. Chu, E. Tiesinga, P. J. Leo, and C. J. Williams, *Phys. Rev. A* **70**, 03701 (2004).
- [16] A. Recati, P. O. Fedichev, W. Zwerger, J. von Delft, and P. Zoller, *Phys. Rev. Lett.* **94**, 040404 (2005).
- [17] R. B. Diener, B. Wu, M. G. Raizen, and Q. Niu, *Phys. Rev. Lett.* **89**, 070401 (2002).
- [18] P. Böhi, M. F. Riedel, J. Hoffrogge, J. Reichel, T. W. Hänsch, and P. Treutlein, *Nature Physics* **5**, 592 (2009).
- [19] N. Schlosser, G. Reymond, I. Protsenko, and P. Grangier, *Nature (London)* **411**, 1024 (2001).
- [20] C.-S. Chuu, F. Schreck, T. P. Meyrath, J. L. Hanssen, G. N. Price, and M. G. Raizen, *Phys. Rev. Lett.* **95**, 260403 (2005).
- [21] A. Steffen, A. Alberti, W. Alt, N. Belmechri, S. Hild, M. Karski, A. Widera, and D. Meschede, *Proceedings of the National Academy of Science* **109**, 9770 (2012).
- [22] I. Fuentes-Guridi, A. Carollo, S. Bose, and V. Vedral, *Phys. Rev. Lett.* **89**, 220404 (2002).
- [23] I. Fuentes-Guridi, S. Bose, and V. Vedral, *Phys. Rev. Lett.* **85**, 5018 (2000).
- [24] E. Martin-Martinez, A. Dragan, R. B. Mann, and I. Fuentes, *ArXiv e-prints* (2011), 1112.3530.
- [25] R. A. Bertlmann, K. Durstberger, Y. Hasegawa, and B. C. Hiesmayr, *Phys. Rev. A* **69**, 032112 (2004).
- [26] P. P. Orth, I. Stanic, and K. Le Hur, *Phys. Rev. A* **77**, 051601(R) (2008).
- [27] M. A. Cirone, G. D. Chiara, G. M. Palma, and A. Recati, *New Journal of Physics* **11**, 103055 (2009).
- [28] M. Bruderer and D. Jaksch, *New Journal of Physics* **8**, 87 (2006), arXiv:quant-ph/0601202.
- [29] W. Hänsel, P. Hommelhoff, T. W. Hänsch, and J. Reichel, *Nature (London)* **413**, 498 (2001).
- [30] T. P. Meyrath, F. Schreck, J. L. Hanssen, C.-S. Chuu, and M. G. Raizen, *Phys. Rev. A* **71**, 041604 (2005).
- [31] A. Sinatra, Y. Castin, and E. Witkowska, *Phys. Rev. A* **75**, 033616 (2007).
- [32] A. Widera, O. Mandel, M. Greiner, S. Kreim, T. W. Hänsch, and I. Bloch, *Phys. Rev. Lett.* **92**, 160406 (2004).
- [33] A. Retzker, J. I. Cirac, M. B. Plenio, and B. Reznik, *Phys. Rev. Lett.* **101**, 110402 (2008).
- [34] E. Martín-Martínez, I. Fuentes, and R. B. Mann, *Phys. Rev. Lett.* **107**, 131301 (2011).
- [35] B. L. E, *Quantum Mechanics: a modern development* (World Scientific Publishing, 1998).
- [36] E. Sjöqvist, A. K. Pati, A. Ekert, J. S. Anandan, M. Ericsson, D. K. L. Oi, and V. Vedral, *Physical Review Letters* **85**, 2845 (2000).
- [37] K. Singh, D. M. Tong, K. Basu, J. L. Chen, and J. F. Du, *Phys. Rev. A* **67**, 032106 (2003).
- [38] V. Giovannetti, S. Lloyd, and L. Maccone, *Nature Photonics* **5**, 222 (2011).
- [39] M. G. A. PARIS, *International Journal of Quantum Information* **07**, 125 (2009).